AUT Journal of Civil Engineering

AUT J. Civil Eng., 10(1) (2026) 25-48
DOI: 10.22060/ajce.2025.24157.5923

Seismic Behavior of Dry Sandy Soils Improved with Block-Type Deep Soil Mixing in Near-Fault Regions

Ali Yaghfoori, Iraj Mahmoudzadeh Kani*, Hassan Yousefi

Department of Civil Engineering, College of Engineering, University of Tehran, Tehran, Iran.

ABSTRACT: Block-Type Deep Soil Mixing (BDSM) method is widely recommended for enhancing soil in sensitive geotechnical projects. Nevertheless, previous studies have predominantly focused on alternative DSM techniques, particularly grid-type methods, with emphasis on liquefaction mitigation, while the dynamic and seismic performance of BDSM—especially under high-frequency and near-fault excitations—has received limited attention. Considering the high-frequency content of nuclear power plant structures and the stiffness enhancement introduced by BDSM, a precise seismic evaluation is essential. This study investigates the seismic response of dry Nevada sand treated with BDSM under Ricker waves and near-fault earthquake records, including scenarios with and without pulse effects. Plane-strain modeling of the sand layer was conducted in GID, and numerical analyses were performed in OpenSees using the PDMY02 constitutive model. Lateral and bottom boundaries were modeled with semi-infinite free-field columns and viscous dampers. Results indicate that BDSM effectively reduces horizontal accelerations at higher frequencies; however, increasing its thickness can amplify vertical accelerations due to rocking. A thickness equivalent to one-fifth of the shear wavelength is recommended as an initial design criterion. While increasing the DSM width has minimal effect on horizontal accelerations, it can moderate vertical rocking-induced responses. The relative density of sand increases horizontal accelerations, whereas its impact on vertical response depends on input frequency and the dynamic properties of both the soil and BDSM. These findings underscore the critical importance of project-specific design and performance evaluation of BDSM, particularly for sensitive, high-frequency structures such as nuclear facilities, to optimize seismic performance and mitigate dynamic effects.

Review History:

Received: May, 15, 2025
Revised: Nov. 23, 2025
Accepted: Dec. 19, 2025
Available Online: Dec. 21, 2025

Keywords:

BDSM
Near-Fault Ground Motions
Bidirectional Loading
Seismic Performance
Rocking Motion

1- Introduction

Deep mixing is an advanced soil improvement technique that stabilizes soft and problematic soils. This method involves stabilizing the soil in situ with binders, such as cement or lime, without compaction. Cement is usually preferred over lime due to its superior mechanical properties. Deep mixing is commonly applied to enhance soft clays and organic soils, aiming to increase bearing capacity, reduce active earth pressure, mitigate settlement, enhance passive earth pressure, and control seepage. It is also used to improve sandy soils, addressing issues such as increased bearing capacity, reduced settlement, prevention of liquefaction, and seepage control [1-7]. Several factors influence the performance of deep-mix-treated soils, including the type of binder, soil properties (particularly clay), and the mixing and curing conditions applied in the field [5, 7]. The deep mixing technique entails mixing natural soil on-site with either slurry (wet method) or powders (dry method) to create enhanced soil columns or panels. The dry method offers advantages such as lower water content, reduced binder usage, and typically higher strength. Conversely, the wet method produces more uniform columns; however, it may not be practical in high-water-content conditions, as a high water-to-binder ratio can weaken the treated soil [8]. Dry soil mixing, which uses a dry admixture, is most effective for soils with a moisture content greater than 60% or those approaching the liquid limit. This method is typically applied to clays, highly organic soils, peats, and other weak soils. In contrast, wet soil mixing is better suited for drier soils that require additional moisture for cementation reactions and can reach depths of up to 30 meters [9]. In recent years, deep soil mixing (DSM) has gained popularity for reinforcing soil foundations due to its ability to increase stability, reduce settlements, minimize environmental impact, speed up execution, lower costs, and enable work at greater depths (over 40 meters) in diverse soil types .[10] In recent decades, numerous studies have focused on laboratory experiments to examine how the type and quantity of binders influence the strength, stiffness, consolidation time, and permeability of soil-binder mixtures 11-15 ,4 ,2 ,1]]. Several studies have also examined factors

*Corresponding author's email: imkani@ut.ac.ir

influencing the field installation of Deep Soil Mixing (DSM), including the number of mixing blades, rotational speed, and other operational parameters [16, 17]. Numerical analyses of building foundations or embankments on soft soils reinforced with Deep Soil Mixing (DSM) often focus on case-study back-analysis, typically using commercial software such as PLAXIS, FLAC, ANSYS, and ABAQUS [18]. Some studies have also investigated the seismic response of reinforced soil systems, assessing the performance of various DSM methods under seismic loading. Thanh Sang To et al. [19] developed a novel back-analysis approach for lateral displacements of DCM columns in deep excavations. By combining a metaheuristic optimization algorithm, 3D PLAXIS simulations, and Python programming, their method accurately predicts stiffness parameters of very soft soils and DCM columns, enabling reliable displacement forecasts and risk assessment while improving safety, efficiency, and underground structure design. Hashminejad et al. investigated the seismic response of shallow foundations on liquefiable soils stabilized with DSM columns. Their findings indicate that increasing the DSM column diameter reduces the risk of liquefaction, while greater horizontal distance from the DSM columns increases this risk. However, as the distance from the DSM column center increases, its effectiveness in mitigating liquefaction significantly diminishes [20]. Ramazani et al. [21]conducted numerical studies on deep soil mixing (DSM) columns and demonstrated that this soil improvement technique can effectively reduce excess pore water pressure. Their results indicated that column arrangement, diameter, height, and the improvement ratio of area significantly influence the seismic performance of foundations. Notably, the individual column arrangement (ICA) outperformed the wall column arrangement (WCA) in mitigating excess pore pressure, with the area improvement ratio being the most critical controlling factor. Bradley et al. studied the effect of different lattice-shaped soil improvement configurations on the seismic response of liquefiable soil deposits through three-dimensional effective stress analysis of sandy soils. Their findings showed that all improved soil geometries effectively mitigated liquefaction, reducing the surrounding soil's peak surface displacements and inferred vertical settlements. They also found that soil improvement increased spectral accelerations for short to moderate vibration periods of ground motion at the surface, implying that structures on improved soils may face higher inertial seismic demands [22]. Dehghan Khalili et al. [23] conducted experimental studies demonstrating that Deep Soil Mixing (DSM) columns can effectively mitigate soil liquefaction and reduce settlements of shallow foundations. Different column arrangements, including square, triangular, and single configurations, significantly influence soil improvement performance, with excess pore water pressure reduced by 20% to 50% compared to untreated soil. Furthermore, the increase in soil shear stiffness induced by DSM columns substantially decreases foundation settlement, with the most effective configuration reducing settlement to approximately 10% of that observed in untreated soil. Song et al. evaluated the seismic performance of T-shaped deep-mixing (TDM) columns compared with conventional deep-mixing (DM) columns in clay layers subjected to embankment loading. Their findings indicated that TDM columns provide a practical, cost-effective, and technologically advanced solution for improving the stability of soft ground under embankment loads, compared with traditional DM columns [24]. Namikawa et al. studied the dynamic behavior of soil-cement-reinforced walls and found that increasing the area of soil improvement significantly enhances the ground's ability to mitigate liquefaction. The elastic modulus of the cement-treated soil is also crucial in this process. While soil-cement-improved walls may experience partial failure during strong earthquakes, such failure does not cause significant displacement of the unimproved soil or compromise liquefaction mitigation unless the failure is severe25]]. Khosravi et al. conducted large-scale centrifuge tests to evaluate the seismic response of grid-type soil-cement reinforcement. They found that unreinforced soil exhibited significant nonlinearity during intense shaking, whereas reinforcement reduced nonlinearity, increased site stiffness, and amplified ground surface accelerations [26]. Yaghfoori et al. [27], in a case study on a nuclear power plant project, used numerical modeling of layered soil improved with Block-Type Deep Soil Mixing (BDSM) under elastic conditions. They showed that increasing the width of BDSM blocks reduces vertical accelerations induced by rocking motion, but further widening beyond 1.5 times the block width has no significant additional effect. Moreover, increasing the block thickness amplifies the rocking motion. The study emphasizes the importance of analyzing the DSM-soil-DSM interaction and highlights the role of rocking motion in transmitting accelerations to the surrounding soil.

Several numerical studies have investigated the distribution of shear stresses and strains in liquefiable soil deposits reinforced with Deep Soil Mixing (DSM) grids, using three-dimensional linear-elastic finite-element analyses of unit cells within the OpenSees PL platform .[28] The selection of column installation patterns is influenced by various factors, such as the size of the superstructure, its intended function, construction costs, and site conditions. Block patterns offer the greatest stability but are the most expensive option. In contrast, grid and wall patterns balance stability and cost-effectiveness, although they demand precision during installation. Block improvements are typically used in large, permanent structures such as breakwaters, power plant foundations, and sea revetments at ports [5, 29]. Most research has concentrated on grid and wall-type deep soil mixing for soil liquefaction mitigation; however, the seismic behavior of block-type DSM, commonly used in large industrial and power plant foundations to manage settlements and reduce site response, remains insufficiently explored. This paper evaluates the seismic performance of sand layers improved using the block deep soil mixing (BDSM) method in a two-dimensional elastoplastic space, utilizing the PDMY02 constitutive model in the OpenSees finite element software. Initially, the effect of the relative density of sand (Nevada) on the seismic performance of DSM is investigated.

Subsequently, the impact of DSM thickness and width on the seismic responses of the improved sand layer will be analyzed. Furthermore, given the high cost of DSM implementation, especially at greater depths, two alternative designs are proposed, and their seismic performance is compared with that of the conventional block deep soil mixing method. Near-fault ground motions, due to the very short distance between the earthquake source and the site, exhibit distinct dynamic characteristics such as large-amplitude velocity pulses caused by forward directivity, permanent displacement (fling step), and unusually high vertical-to-horizontal acceleration ratios [30-32]. These features can subject soil–structure systems—particularly stiff and heavy structures as well as ground-improvement systems such as Deep Soil Mixing (DSM)—to intense rocking motions, amplified vertical response, and significant variations in input energy. In this study, a suite of near-fault earthquake records was employed to evaluate the seismic behavior of sand improved with the Block-type DSM technique, thereby enabling a realistic and critical assessment of the system's performance under such demanding loading. The importance of examining near-fault motions stems from the fact that structures and geotechnical improvement systems located within a few kilometers of the fault are most vulnerable to these velocity pulses and elevated vertical accelerations. Accordingly, accurately analyzing and understanding the dynamic response of the soil–DSM system under near-fault earthquakes is essential for safe design and risk assessment in critical projects.

2- Numerical modeling

This study analyzed a two-dimensional elastoplastic finite-element model of sandy soil using OpenSees V3.5.0. OpenSees provides practical tools for analyzing structural and geotechnical systems in engineering applications [33]. GiD 14.0.1 was used for preprocessing and postprocessing tasks [34]. Figure 1 illustrates a numerical model of dry Nevada sand measuring 400 m by 150 m, which was developed. The sand was improved using the block-type deep mixing (DSM) technique, and its seismic response was assessed under vertical Ricker wavelet excitation and near-fault earthquakes. For soil modeling, 4-node quadrilateral elements were utilized. Nonlinear finite element analyses were conducted with the single-phase version of the pressure-dependent, multi-yield (PDMY02) Constitutive model implemented in OpenSees [28, 35-38]. This model is based on multi-yield-surface plasticity, employing conical yield surfaces with varying tangent moduli to capture shear stress-strain nonlinearity and confinement-dependent shear strength. For most soils, small-strain damping has a finite non-zero value [39, 40]. Laboratory and field data indicate that for sands such as Nevada Sand, the small-strain damping ratio typically ranges from 0.9% to 2.6% [41]. Inverse analyses of vertical array records from the 1995 Kobe earthquake by Kokusho et al. [42, 43], as well as back-calculated profiles by Park and Hashash [41] for the Mississippi Embayment, show a similar trend, with small-strain damping values around 3–3.5%. Based on this information, a small-strain damping range of 1–4% was adopted in the present study. For example, Deng et al. [44] used a 2% small-strain damping for dry Nevada Sand in finite element analyses of underground structures. Pressure-dependent constitutive models such as PDMY02 behave nearly linearly at small cyclic strains. Thus, the hysteretic damping produced at these strain levels is negligible (less than 0.04% for shear strains of 0.01–0.02%), which is far below the damping observed in laboratory tests. To compensate for this deficit and reproduce the energy dissipation of real soils at small strains, Rayleigh viscous damping is typically added to the model. This not only reproduces small-strain damping accurately but also improves numerical stability and prevents significant errors in the results, even at higher levels of shaking and larger strains. Without viscous damping, the numerical model cannot capture the soil's actual small-strain behavior, leading to inaccurate dynamic simulations. Rayleigh damping with 2% damping was applied at low strain levels [44]. Table 1 provides the specifications of the DSM used in this study, and Table 2 summarizes the geotechnical properties of Nevada sand at different relative densities [44, 45].

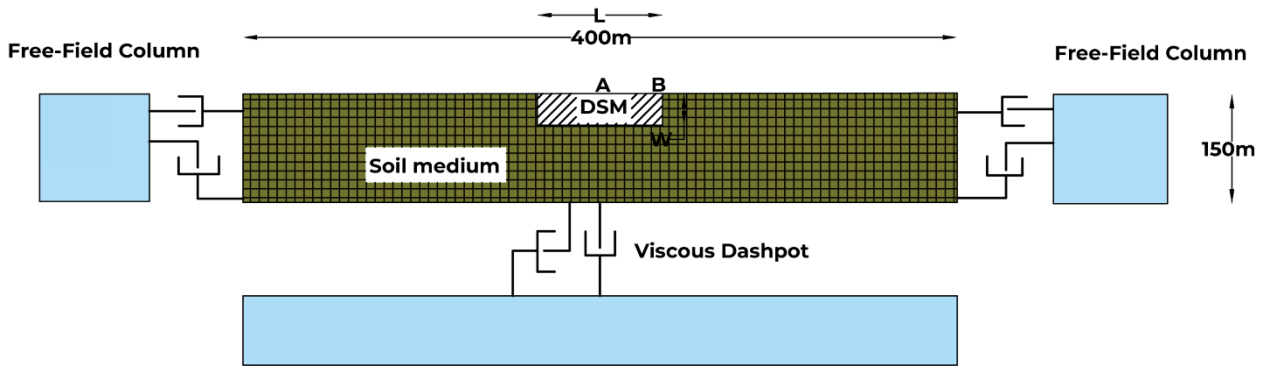

Fig. 1. Model Geometry.

Table 1. Properties of improved soil.

Density(t/m$^{3)}$	S-Wave Velocity(m/s)	P-Wave Velocity(m/s)
2.3	1300	2400

Table 2. Summary of PDMY model parameters for Nevada sand [44].

Parameter	Value					Unit	Description
D_r	60	61	64	69	74	%	Relative density
e	0.67	0.67	0.66	0.65	0.64	-	Void ratio
ρ	1.59	1.59	1.6	1.61	1.62	ton / m^3	Unit weight
ρ'_r	101	101	101	101	101	kPa	Reference effective confining pressure
$G_{max,1,oct}$	68.95	70.25	73.42	78.23	83.86	MPa	Octahedral low-strain shear modulus
$\gamma_{max,r}$	0.1	0.1	0.1	0.1	0.1	-	Maximum octahedral shear strain
B_r	184.09	187.57	196.06	208.91	223.95	MPa	Bulk modulus
d	0.5	0.5	0.5	0.5	0.5	-	Pressure dependency coefficient
φ_{TXC}	34.3	34.3	34.8	36.2	37.1	deg.	Triaxial friction angle used by the model
φ_{PT}	26.3	26.3	26.4	26	26.1	deg.	Phase transformation angle
C_1	0.04	0.042	0.036	0.02	0.019	-	Control the shear-induced volumetric change and contraction tendency.
C_2	2.85	2.72	2.3	1.5	1.49	-	On the dilation history and the overburden stress effect, respectively.
C_3	0.21	0.21	0.19	0.15	0.15	-	
d_1	0.07	0.07	0.09	0.15	0.18	-	Reflect dilation tendency, stress history, and overburden stress, respectively.
d_2	3	3	3	3	3	-	
d_3	0	0	0	0	0	-	
NYS	20	20	20	20	20	-	Number of yield surfaces generated by the model
liq_1	1	1	1	1	1	-	Account for permanent shear strain (slip strain or cyclic mobility)
liq_2	0	0	0	0	0	-	

An absorbing boundary was defined along the lateral and bottom edges of the model using the ASDAbsorbingBoundary2D command, accounting for soil layer characteristics at each boundary level. To simulate the interaction between adjacent improved and natural soil blocks, the degrees of freedom of the improved and natural soil were constrained in the vertical and horizontal directions using the equal command. A time-history analysis was conducted using a constant time step and the penalty method to enforce the constraint equations. The Krylov-Newton method was selected as the solution algorithm, and convergence was tested using the Norm Displacement Increment Test with a tolerance. The RCM numberer, based on the reverse Cuthill-McKee method, was applied to relate equation numbers to degrees of freedom. The TRBDF2 integrator, a hybrid method combining the trapezoidal rule and the three-point backward Euler method, was employed [33, 35].

2- 1- Mesh size and time step

The precision of numerical simulations in seismic wave propagation related to dynamic soil-foundation interaction (SSI) issues is mainly influenced by two essential factors: element size (Δh) and time step (Δt). The soil element size (Δh) is determined according to the Courant-Friedrichs-

Lewy (CFL) condition, which dictates that it should not exceed one-tenth of the shortest wavelength (λ_{min}) [46-49]. To accurately represent a traveling wave of a given frequency, at least 10 nodes per wavelength are required. Using fewer than 10 nodes can lead to numerical damping because the discretization may miss some peaks of the seismic waves [48].

$$\Delta h \le \Delta h_{\max} = \frac{\lambda_{\min}}{10} = \frac{C_{\min}}{10 f_{\max}} \quad (1)$$

The second stability criterion is closely related to the principles of the finite element method. As a wavefront propagates through space, it reaches each node sequentially. Suppose the time step in finite element analysis is too large. In that case, the wavefront may reach two consecutive nodes simultaneously, violating the fundamental principle of wave propagation and potentially causing instability. Therefore, the time step must be carefully managed to ensure stability [48, 49]. In this study, the time step (Δt) was selected to be smaller than the ratio of the smallest element size to the maximum wave velocity of the soil.

$$\Delta t \le \frac{\Delta h}{C_{\max}} \quad (2)$$

where (C_{max}) represents the maximum wave velocity in the soil. The element size and time step were determined based on the soil-layer characteristics and the selected Ricker-wave or earthquake frequency, as required for each analysis in this study. The input excitation was applied as velocity components at the model's lowest boundary, vertically and horizontally, and simultaneously in both directions.

2- 2- Boundary Condition

Since the model represents only a portion of the soil, artificial boundaries must be established around it. While constraining the degrees of freedom at these boundaries is adequate for static analyses, it can lead to wave reflections in dynamic analyses. To address this issue, peripheral boundaries can be placed sufficiently far from the main soil area; however, this increases both analysis time and computational cost. Various methods have been proposed for modeling absorbing boundaries. In the present study, Nielsen's methodology is implemented to model absorbing boundaries surrounding the soil domain, thereby minimizing reflection of seismic waves at the model edges and accurately representing wave propagation in a semi-infinite medium. This method, applicable in two- and three-dimensional settings, is illustrated in Figure 7. In this diagram, F represents the free field, which is analyzed parallel to the primary soil environment; D stands for the Lysmer-Kuhlemeyer dampers that absorb outgoing waves; and T denotes the boundary forces transferred from the free field to the main soil environment, conveyed through this mechanism [47, 50, 51].

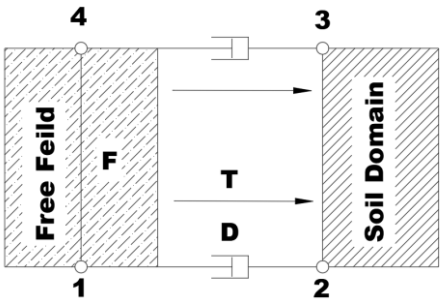

Fig. 2. A schematic representation of the three key components of an absorbing element [51, 52].

2- 3- DSM-Soil interface

In the 2D finite element model, DSM blocks were modeled using four-node quadrilateral (quad) elements under plane strain, with linear-elastic behavior. This method follows common practice in seismic analysis of DSM, in which DSM columns are often modeled as a continuous medium with simplified material properties, thereby supporting the validity of our model [18, 22]. The soil–structure interface plays a critical role in accurately simulating real-field soil–structure interaction (SSI) mechanisms, as the foundation interacts with the surrounding soil at this interface. Two primary types of interfaces commonly used in nuclear power plant analyses are tied/bonded and nonlinear/unbonded. The tied interface represents the simplest form, in which no separation or gapping occurs, thereby ensuring synchronized behavior of the foundation and soil during dynamic events. In contrast, the nonlinear interface simulates the realistic seismic behavior of soil, allowing sliding and small gaps between the foundation and soil. This feature enables modeling of rocking motion in shallow foundations, a key aspect of SSI for estimating seismic responses [53]. Although nonlinear interfaces are generally expected to reduce structural seismic responses, this is not universally true; incorrect interface specifications may lead to inaccurate seismic demand estimates, potentially jeopardizing safety-critical structures such as NPPs [54, 55]. Previous studies have demonstrated that the interface's effects on structural acceleration and displacement depend on the soil type and earthquake frequency. Nguyen et al. [55] showed that, except for very stiff soils (S1), the roof acceleration is not significantly affected whether a fully bonded or nonlinear interface is assumed; thus, in most cases, nonlinear interface behavior can be neglected. However, for low to medium-frequency earthquakes across all soil types, a sliding interface can increase displacements compared to a fully bonded interface. Sextos et al. [56] reported that containment buildings on soft soil are more susceptible to uplift and combined nonlinear phenomena such as sliding and rocking, particularly in response to seismic pulses within the 0.5–1.0 Hz frequency range. Saxena et al. [57, 58] further showed that sliding and gapping at the interface increase structural stresses, with the intensity dependent on the friction

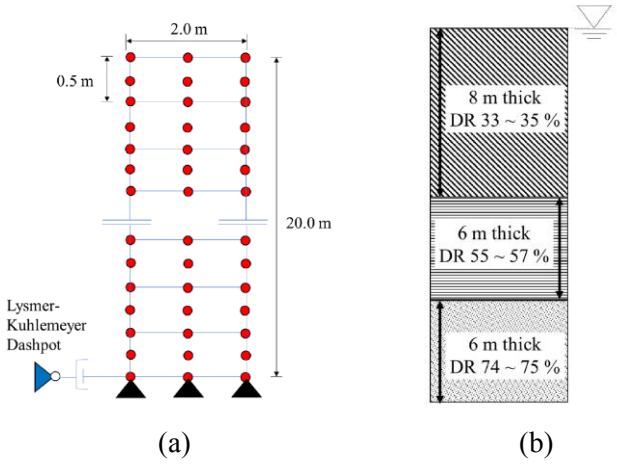

Fig. 3. The numerical model used in the current study. (a) element and mesh; (b) soil profile[59].

coefficient and the foundation embedment depth. Increasing the foundation depth can mitigate the effects of sliding and gapping. Kanellopoulos et al. [54], in a 3D reactor model of a 34.5 m-thick layered soil, demonstrated that gapping mechanisms can generate higher-frequency excitations that can adversely affect internal structural components, such as the reactor containment. Therefore, the DSM–soil interface, a pivotal aspect of this study, may affect the structure's seismic response. This impact is contingent on project-specific conditions or finite-element modeling choices. However, a more robust implementation of the DSM can help alleviate these effects. Given the FE modeling conditions, substantial foundation embedment, and the DSM application—which previous studies indicate can mitigate sliding and gapping at the soil–foundation interface—along with OpenSees software limitations in the pre-processing stage, all interface nodes were tied in all directions in this study to facilitate comprehensive analyses. It should be noted that this study does not aim to provide a general analytical methodology covering all aspects of DSM-Soil interaction; instead, it emphasizes the importance of DSM-Soil interaction and examines the overall effect of block-type deep soil mixing, which is generally applicable.

3- Model validation

3- 1- Benchmark 1

Gupta et al. studied liquefaction in a two-dimensional plane-strain environment. [59]. OpenSees software was employed to model the saturated sand layers. The modeling was performed according to3 [59, 60] . The geometry was modeled using 9-node quadrilateral elements, and the sand's behavior was simulated using the PDMY03 model. The lateral boundaries were periodic, while the lower boundary was modeled using the Lysmer-Kuhlemeyer method absorber. The groundwater table was presumed to align with the ground surface. According to Figure 4, the ground motion record from the Imperial Valley (1979) was scaled to an acceleration

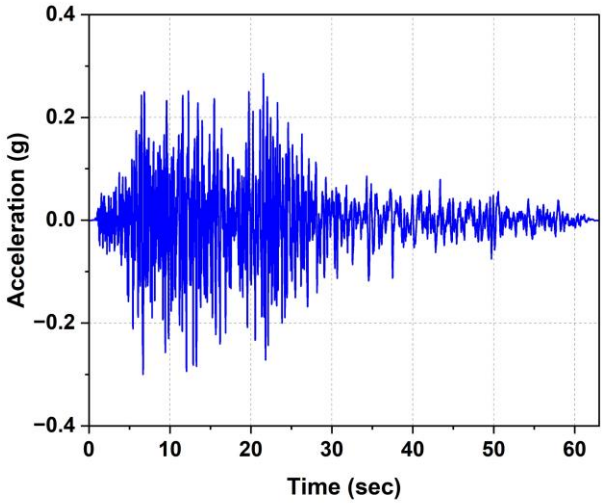

Fig. 4. Earthquake records - scaled to 0.3g(Imperial Valley (1979)).

of 0.3g for the analysis. Under the conditions established in the study, the analysis results using 4-node quadrilateral elements are shown in Figure 5.

We have quantified the agreement between the developed model and the baseline data using percentage-based metrics. The Mean Absolute Percentage Error (MAPE) was calculated to quantify the relative point-by-point deviation between the model outputs and the baseline values. Furthermore, the percentage of samples with less than 5% deviation from the baseline was determined, providing a direct measure of the proportion of predictions falling within an acceptable accuracy range. An overall agreement metric, defined as the ratio of the mean difference to the mean baseline value, was also introduced; higher values indicate greater similarity to the reference data. All of these percentage-based metrics are

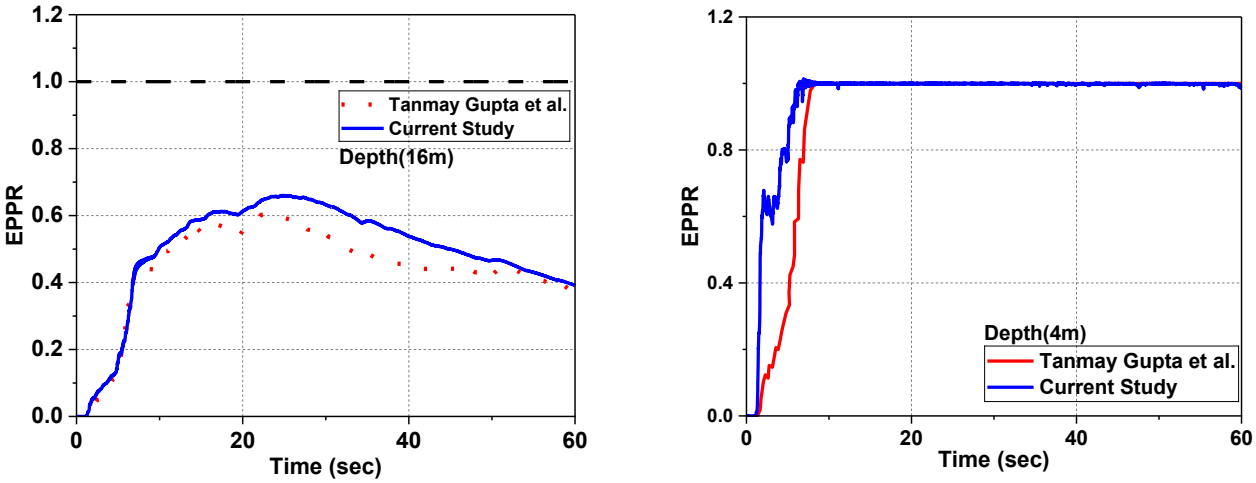

Fig. 5. EPPR response of the soil column subjected to the Imperial Valley earthquake, considering [59].

Table 3. Percentage-Based Evaluation of Model Agreement with Baseline Data (Excess Pore Water Pressure at 16 m Depth)

MAE	RMSE	MAPE (%)	Similarity (%)	Within 5%
0.043429	0.13779	21.116	95.507	88.669

summarized in Table 3 for the excess pore pressure at a depth of 16m.

3- 2- Benchmark 2

Camilo et al. investigated free-field lateral spreading using centrifuge testing and two numerical models in the OpenSees software. [41]. The first numerical model consisted of 2,680 nodes and 2,113 BrickUP elements in three dimensions. Because the first model was computationally expensive, it was assumed that modeling a cantilever beam in three-dimensional space, as shown in Figure 6, would enable simulation of the centrifuge test results and evaluation of free-field lateral spreading with less computational cost. This model consisted of 40 nodes and 9 BrickUP elements in three-dimensional space. This model constrained degrees of freedom in the x, y, and z directions for nodes at the same height. At the lower boundary of the model, all degrees of freedom of the nodes were fixed. Nevada sand with a density range of 45-35% was used in the numerical model. The PDMY model, as specified in Table 4, was used to simulate the behavior of saturated sand. The model was analyzed using the earthquake record shown in Figure 7. The results from the analysis and simulations conducted in this study for ($\zeta_{small\ strain} = 1.0\%$) are shown in Figure 8.

The Percentage-Based Evaluation of Model Agreement with Baseline Data for Surface Displacement is Presented in Table 5.

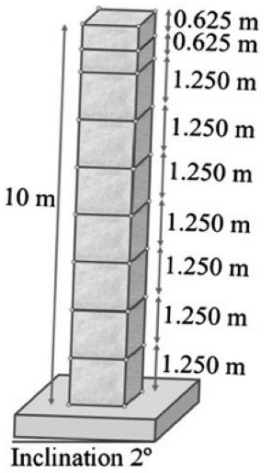

Fig. 6. Soil profile geometry[41].

4- Impact of Soil Domain Size on Seismic Response: Sensitivity Study

One factor affecting the accuracy of seismic analyses is the selection of an appropriately sized soil domain relative to the foundation dimensions. For instance, the ASCE/SEI 4-16: Seismic Analysis of Safety-Related Nuclear Structures code states that, in finite element analyses considering soil-structure interaction, viscous dashpots oriented normal and

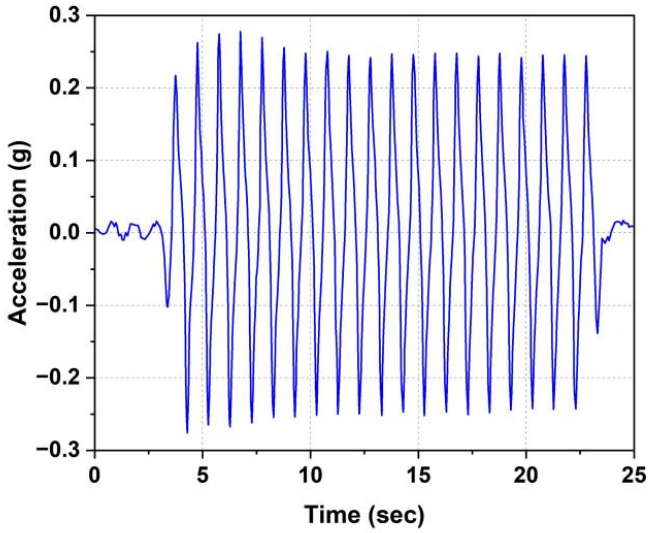

Fig. 7. Input acceleration time history applied at the base of experiment I-02 [41].

Table 4. Effective stress constitutive model parameters for Nevada Sand (D_r=35-45%) [41].

Variable	Value	Units
Mass density	19.8	kg/m^3
Ref. shear modulus	33000	kPa
Ref. mean confinement	80	kPa
Confinement dependence coeff	0.5	Dimensionless
Friction angle	31.4	degree
Peak shear strain	10	%
Number of Yield Surfaces	20	Dimensionless
Phase transformation angle	26.5	degree
Contraction parameter, $\boldsymbol{c_1}$	0.11	Dimensionless
Dilation parameter 1, $\boldsymbol{d_1}$	0.3	Dimensionless
Dilation parameter 2, $\boldsymbol{d_2}$	1	Dimensionless
Liquefaction Parameter, $\boldsymbol{\gamma_y}$	0.01	Dimensionless
Permeability coefficient	0.003	m/s

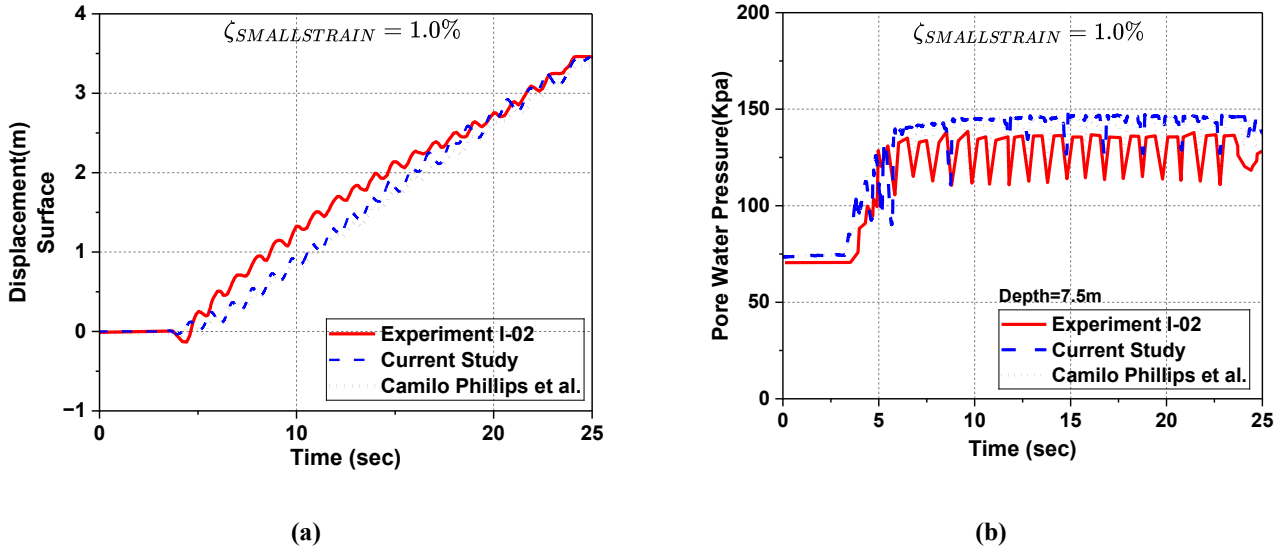

Fig. 8. (a) Comparison of boundary displacements for numerical simulations and centrifuge experiment I-02; (b) Comparison of pore water pressure time history for numerical simulations and centrifuge experiment I-02 [41].

Table 5. Percentage-Based Evaluation of Model Agreement with Baseline Data (Displacement at surface).

MAE	RMSE	MAPE (%)	Similarity (%)	Within 5%
0.078272	0.096724	-	94.936	39.469

tangential to the lateral boundaries should be placed at a distance of at least four to five radii from the edge of the structure [49, 61]. These boundaries are not perfect, and their effectiveness decreases when waves approach them at an angle. This recommendation applies when the model boundaries are simulated using only Lysmer–Kuhlmeyer dashpots. In this study, as described in Section 2-2 and schematically illustrated in Figures 1 and 2, a combination of free-field columns and Lysmer–Kuhlmeyer dashpots was employed at the lateral and bottom boundaries, yielding a more effective absorbing boundary. A sensitivity analysis was conducted by increasing the model dimensions, including a deep-mixing soil block width of 80 m and soil-domain dimensions of 400×150 m and 600×150 m, for Nevada sand with a relative density of 60% under one-directional seismic loading from Parkfield-02, CA (2004) (according to Table 7). The results, as shown in Figure 9, indicate excellent agreement in the seismic response of the improved soil. Based on these results and to reduce computational costs, the dimensions of 400×150 m were selected as the basis for modeling and analysis.

5- Results

5- 1- Effect of relative density of sand on the performance of improved soils

The effect of relative density on Deep Soil Mixing (DSM) performance, with dimensions of 83 m × 7.5 m, has been investigated under the vertical Parkfield-02, CA (2004) earthquake, based on the specifications provided in Table 7. Figure 10a illustrates that as the relative density of sand increases, the horizontal responses recorded on the DSM and at point A also increase. The influence of relative density on the horizontal acceleration response spectrum is more pronounced, particularly at higher frequencies. Figure 10b presents the Fourier amplitude spectrum of horizontal acceleration at point A. At frequencies below 0.6 Hz, relative density has no significant effect on the DSM's horizontal acceleration amplitude. However, within the 0.6–1 Hz frequency range, an increase in relative density reduces acceleration amplitude. In contrast, a higher relative density at frequencies above 1 Hz yields a greater horizontal acceleration amplitude at point A. The block Deep Soil Mixing (DSM) method improves soil quality and significantly reduces ground surface responses, particularly when there

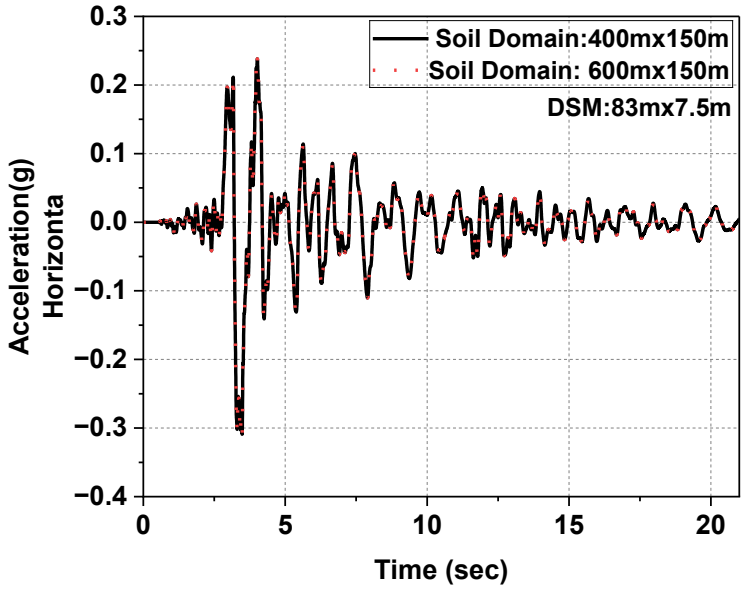

Fig. 9. Consistency of Deep Mixing Soil Response across Different Model Dimensions.

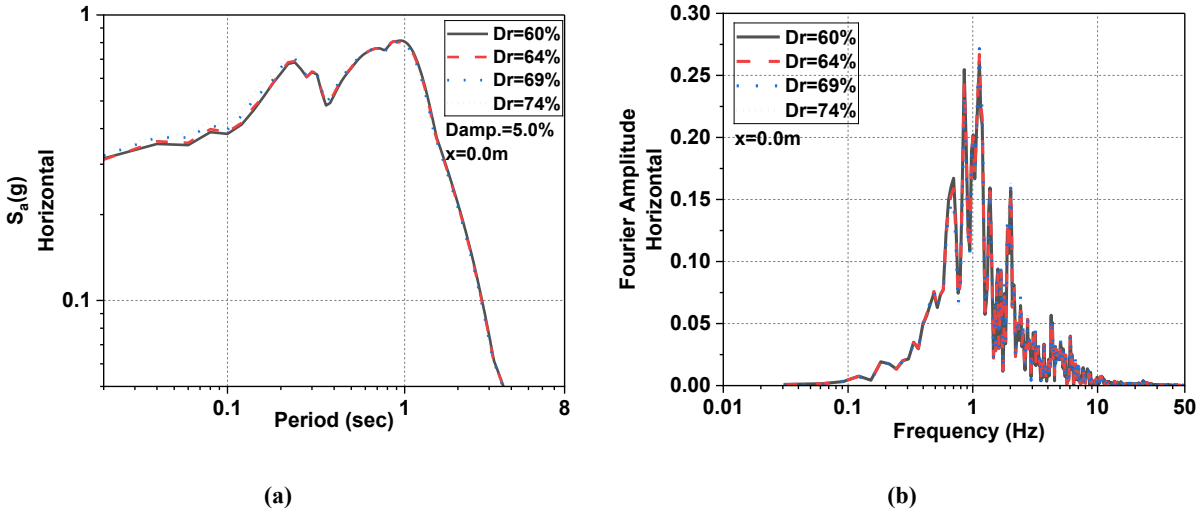

Fig. 10. The effect of relative density on the horizontal responses recorded at point A on the DSM: (a) Horizontal response spectrum acceleration; (b) Fourier amplitude.

is a substantial stiffness contrast between the DSM and the surrounding soil. In other words, the DSM must behave as a rigid block. The high density and volume of the DSM, along with its considerable stiffness relative to the surrounding soil, induce rocking motion. This motion generates significant vertical accelerations on the ground surface, amplifying horizontal accelerations at elevated levels of structures built on it. Both forms of acceleration can adversely affect the performance of structures or delicate equipment situated on the surface of the DSM. Figure 11a presents the vertical-acceleration response spectrum for rocking motion at point B for different relative sand densities. The results indicate that the vertical acceleration spectrum decreases as the sand's relative density increases at periods below 0.1 seconds and above 0.2 seconds. However, higher-density sand exhibits a larger response within the 0.1–0.2 second range.

Figure 11b illustrates the Fourier amplitude spectrum of vertical acceleration due to rocking motion at point B. The results show that for frequencies below 2 Hz, lower-density sand produces greater vertical acceleration amplitudes, whereas for frequencies above 2 Hz, higher-density sand results in larger vertical acceleration amplitudes. It can be concluded that increasing the relative sand density does not yield a consistent pattern in the variations in vertical

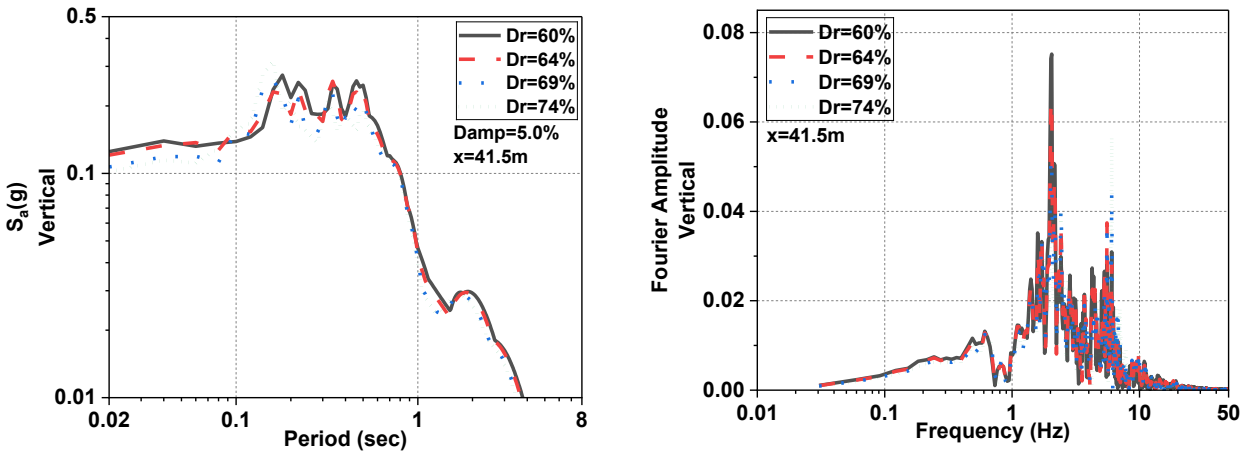

(a) (b)

Fig. 11. Influence of sand relative density on vertical acceleration caused by rocking motion at 41.5 meters from the DSM center. (a) Vertical response spectrum acceleration; (b) Fourier amplitude.

acceleration induced by rocking motion. The seismic performance of DSM is highly dependent on the earthquake's frequency content and the soil's dynamic characteristics.

5- 2- The effect of DSM thickness

The effect of the DSM layer thickness (83 meters wide) on the seismic performance of treated sand has been investigated. In this analysis, the sand relative density is 60%, and the soil profile is analyzed for the Parkfield-02, CA (2004) earthquake. Figure 12b shows that increasing the thickness of the DSM layer reduces the horizontal acceleration at point A, particularly at high frequencies. This reduction is also observed in the velocity and displacement response spectra; however, the effect of DSM on the horizontal acceleration spectrum is more pronounced. Figure 12e presents the Fourier amplitude spectrum of horizontal acceleration at point A for different DSM thicknesses. The results indicate that the DSM layer is more effective in reducing acceleration amplitude at higher frequencies. Specifically, for frequencies above 2 Hz, the reduction in acceleration amplitude becomes significantly more pronounced. Moreover, Figure 12f shows that as the DSM thickness increases, the slope of the Arias intensity curve rises during the first 5 seconds of earthquake loading. This aspect is crucial for structures with high-frequency content. Another key consideration is evaluating whether the seismic performance improvement from increasing the DSM thickness from 10 to 40 meters is justified relative to the additional implementation costs at greater depths. This underscores the need to optimize DSM thickness selection to balance performance and cost-effectiveness.

The effect of DSM thickness on the vertical acceleration induced by rocking motion at a distance of 41.5 meters from the DSM center (point B) is illustrated in Figure 13. Overall, the results indicate that increasing the DSM thickness amplifies the rocking motion within less than 0.1 seconds. Additionally, at a period of 0.18 seconds, the seismic response of the 10-meter-thick DSM is greater than that of the 20 and 30-meter-thick DSM layers. The results showed that increasing thickness and stiffness due to block deep mixing (DSM) increases the soil shear modulus and shear-wave velocity, thereby shifting the frequency content of the soil–structure system toward higher frequencies. This frequency shift near the fault can cause severe rocking motions and an increase in the resulting vertical acceleration. These effects are particularly significant for power plant structures and sensitive equipment with high-frequency content, as increased vertical acceleration can pose substantial seismic hazards. Therefore, a detailed analysis and consideration of DSM effects on soil–structure interaction, especially in fault-near regions and for sensitive structures, are essential.

Analyses revealed that increasing the DSM thickness can reduce horizontal ground accelerations. However, as the thickness increases, particularly at high frequencies, rocking motion and the resulting vertical accelerations tend to intensify. This phenomenon can be particularly significant for power plant structures with high-frequency characteristics, mainly located in near-fault zones. To determine the optimal depth range for deep mixing using the block method, Nevada sand with a relative density of 60% was analyzed under excitation along the x-axis using a Ricker wave with an amplitude of 1g and a frequency of 5 Hz. Figure 14a illustrates the percentage reduction in peak horizontal accelera, on on the DSM at $\boldsymbol{x} = 0.0\ \boldsymbol{m}$. In comparison, Figure 14b presents the percentage increase in peak vertical acceleration due to rocking motion at $\boldsymbol{x} = 41.5\ \boldsymbol{m}$ from the DSM center. In Figure 14a, the values are compared to the free-field response (without DSM), whereas in Figure 14b, they are compared to the response of a DSM with a 7.5-meter thickness. In all cases, the DSM width is 83 meters, and the models were analyzed under a vertical Ricker wavelet with an amplitude

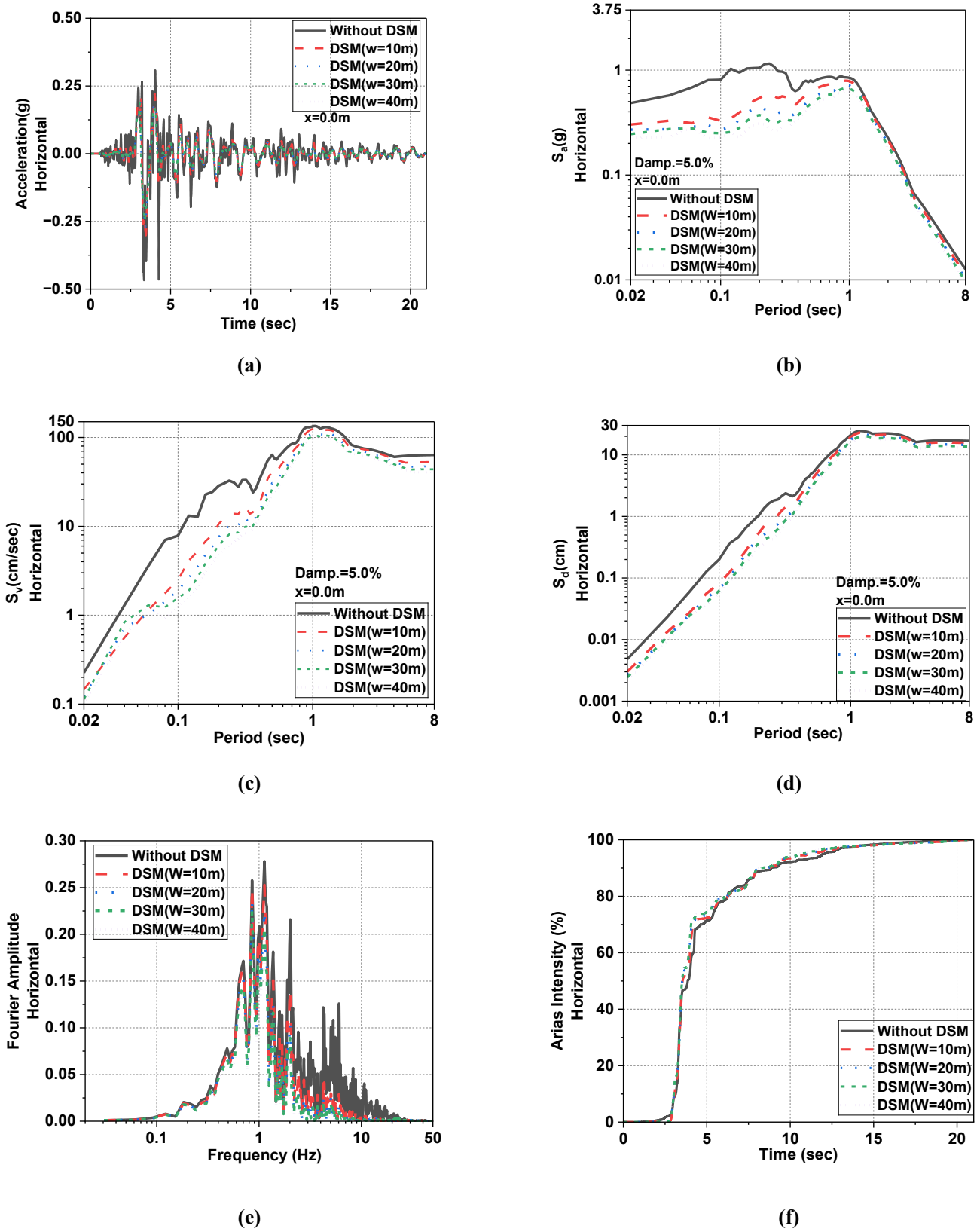

Fig. 12. Response spectrum on the 83-meter-wide DSM Parkfield-02, CA (2004) earthquake. (a) Horizontal acceleration, (b) Acceleration response spectrum, (c) Velocity response spectrum, (d) Displacement response spectrum, (e) Fourier amplitude, (f) Aras intensity.

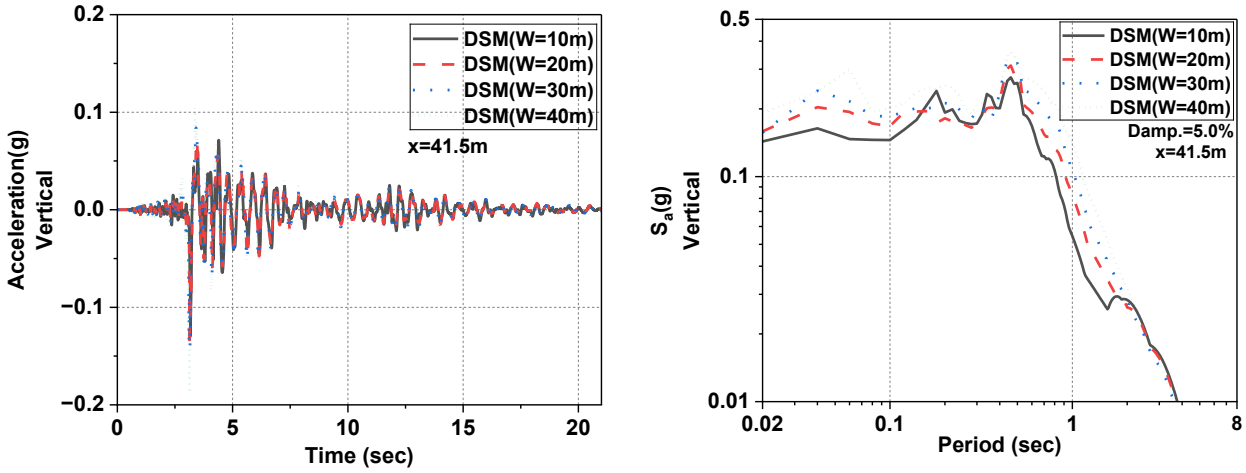

Fig. 13. (a) Vertical acceleration, (b)Vertical acceleration response spectrum due to rocking motion recorded at 41.5 meters from the center of the 83-meter-wide DSM.

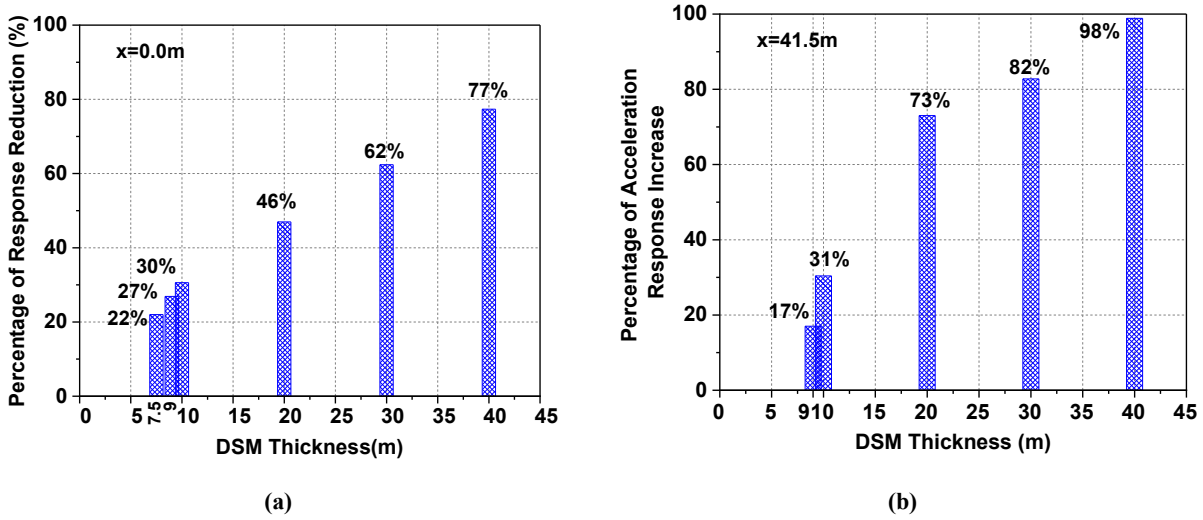

Fig. 14. Effect of DSM thickness on the: (a)reduction of horizontal acceleration at the center of DSM; (b) the increase in vertical acceleration due to rocking motion at a distance of 41.5 meters from the center of DSM.

of 1g and a frequency of 5 Hz. Figures 14a and 14b allow analysis within two DSM thickness ranges: less than 10 meters and greater than 10 meters. For thicknesses exceeding 10 meters, increasing the DSM thickness reduces horizontal acceleration, and extending it to 40 meters has a significant impact on mitigating horizontal acceleration. However, vertical accelerations due to rocking motion increase sharply. This indicates that implementing improved soil layers thicker than 10 meters is not reasonable for the analyzed model. For thicknesses less than 10 meters, increasing the DSM thickness from 7.5 meters to 9 meters and from 9 meters to 10 meters results in a 5% and 3% reduction in horizontal acceleration, respectively. However, the percentage increase in vertical acceleration due to rocking motion for the same thickness increments is 17% and 14%, respectively. Since both the vertical accelerations due to rocking motion and the associated horizontal accelerations—especially in high-frequency ranges—can adversely affect the performance of the structure and its equipment, increasing the DSM thickness beyond 8 meters is not advisable for the analyzed model. In the numerical model, Nevada sand was assumed to have a relative density of 60%, with a Ricker wave frequency of 5 Hz. Accordingly, the shear wave velocity in this sand is 208 m/s, resulting in a shear wavelength of 41 meters. Given the adequate depth of 8 meters for improved soil in this analysis, a depth of one-fifth of the shear wavelength can be

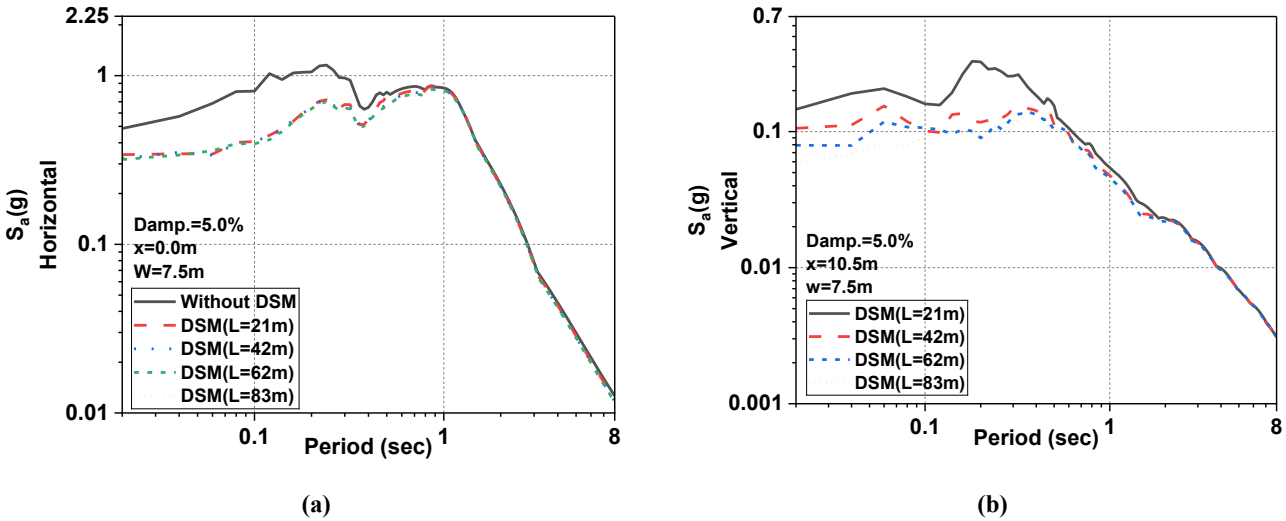

Fig. 15. Effect of DSM width on acceleration response. (a) Horizontal acceleration spectrum at the center; (b) Vertical acceleration spectrum at a distance of 10.5 meters from the center of DSM.

recommended as the optimal DSM depth. It should be noted that this value is proposed as an initial guideline. For each project, a comprehensive soil-structure-DSM interaction study should be conducted, considering the site's soil profile, the structure of interest, and the seismic characteristics of the location to assess the adequacy of the proposed optimal depth.

5- 3- The effect of DSM width

By modeling the DSM with a thickness of 7.5 meters and widths of L = 21, 42, 62, and 83 meters, the effect of DSM width under x-direction excitation for the Parkfield-02, CA (2004) earthquake was analyzed. Figure 15a presents the horizontal acceleration response spectrum at the DSM center. In contrast, Figure 15b illustrates the vertical acceleration response spectrum induced by rocking motion at 10.5 meters from the DSM center. Figure 15a indicates that increasing the DSM width has no significant effect on the horizontal acceleration at its center, as the response spectra for all DSM widths nearly overlap. In contrast, Figure 15b demonstrates that as the DSM width increases, the vertical acceleration induced by rocking motion at 10.5 meters from the DSM center decreases. Therefore, it can be concluded that while the DSM width does not influence horizontal acceleration within the DSM, increasing its width effectively reduces rocking motion and the resulting vertical accelerations.

5- 4- Analysis of lattice arrangement

Studies conducted by Bruce et al. and the FHWA report indicate that the primary factor determining the cost of the deep mixing method is the binder consumption, which depends on soil type, target strength, mixing depth, and project scale [62]. According to the FHWA report, the average cost of stabilizing inorganic soils is approximately 77 USD per cubic yard (≈101 USD/m³). In soils containing organic materials, due to increased binder demand and interference with the cementation process, execution costs increase by an average of 30 USD per cubic yard (≈39 USD/m³). Furthermore, field surveys of contractors indicate that the actual cost of deep mixing can range from 50 to 400 USD per cubic yard (≈65 to 523 USD/m³), driven mainly by treatment depth, required final strength, project volume, site logistics, and schedule constraints. Results reported by Bruce et al. also emphasize that cost variations are more influenced by target strength and project conditions than by the difference between dry and wet mixing methods. [62, 63]. Given the high cost of implementing deep mixing using the block method, two alternative designs were analyzed, as shown in Figure 16. The DSM width was 83 meters in both Model I and Model II. The studied soil profile consisted of dry Nevada sand with a relative density of 60%, and the models were subjected to vertical excitation from the Parkfield-02, CA (2004) earthquake.

Figure 16 illustrates the horizontal acceleration response spectrum at the DSM center and the vertical acceleration response spectrum induced by rocking motion at 41.5 meters from the DSM center. As shown in Figure 17a, Model I and Model II effectively reduce horizontal accelerations within the DSM. However, Figure 17b indicates that both models have higher vertical accelerations due to rocking motion than the block-method DSM implementation. This increase is particularly noticeable for periods shorter than 0.14 seconds and is likely associated with variations in the stiffness and inertial properties of the improved soil. These findings suggest that while the proposed DSM models enhance horizontal acceleration mitigation, they may also introduce unintended vertical accelerations at short periods. This effect is particularly critical for high-frequency structures, such as power plants and vibration-sensitive industrial facilities,

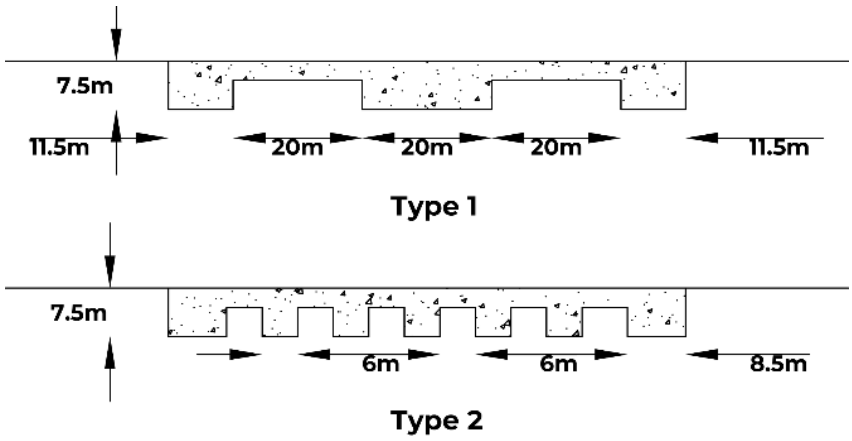

Fig. 16. DSM models are alternatives to block deep mixing.

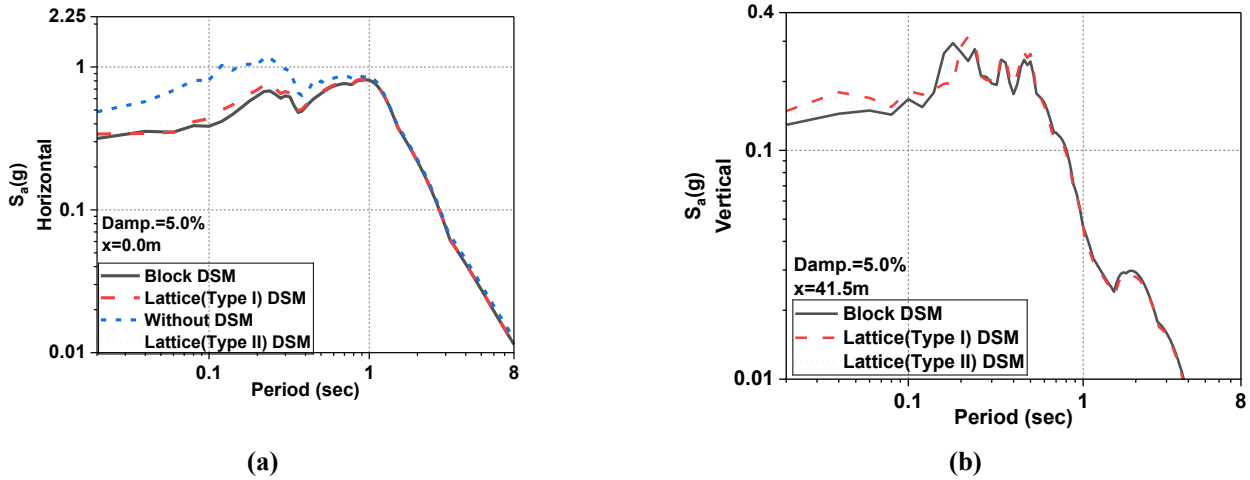

Fig. 17. Acceleration response spectrum on DSM. (a) horizontal acceleration spectrum at the center of DSM; (b) vertical acceleration spectrum due to rocking motion at a distance of 41.5 meters from the center of DSM.

Table 6. Characteristics of the earthquakes used in the bidirectional analysis.

Earthquake name	Station name	M	Site	R_{jb} (Km)	PGA(g) Horizontal	PGA(g) Vertical	Pulse	Forward directivity
Imperial Valley	Holtville Post	6.83	Stiff Sand	5.35	0.258	0.257	yes	yes

where excessive vertical motion can induce resonance and compromise structural performance.

5- 5- The effect of near-fault, bidirectional earthquake loading

In near-fault regions, structures are likely to be subjected simultaneously to both vertical and horizontal components of the earthquake. Therefore, in this section, the performance of the soil profile under bidirectional earthquake loading is evaluated using deep soil mixing (DSM). In this analysis, a semi-infinite layer of Nevada sand with a relative density of 60% and dimensions of , along with DSM blocks measuring $83\ \boldsymbol{m} \times 7.5\ \boldsymbol{m}$, was subjected to the Imperial Valley near-fault earthquake, as specified in Table 6.

In Figure 18a, the Fourier amplitude spectrum of

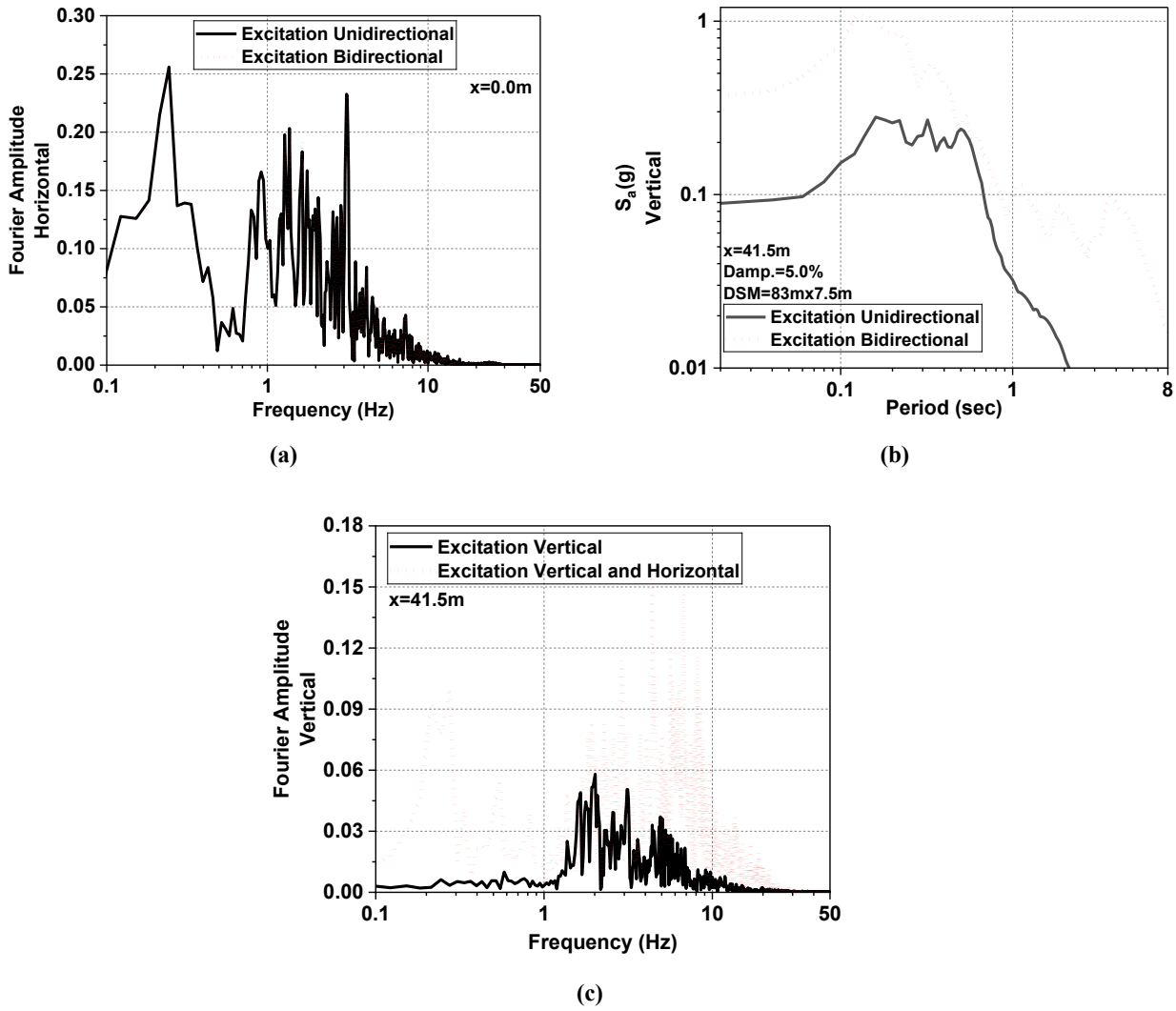

Fig. 18. Figure 5-10. Effect of bidirectional seismic loading: (a) horizontal acceleration response spectrum at the center of the DSM block, and (b) vertical acceleration response spectrum at a distance of 41.5 m from the DSM center.

horizontal acceleration at the center of the DSM (x = 0.0 m) is shown for two earthquake loading scenarios (single-directional and bi-directional). The results indicate that applying the earthquake simultaneously in both horizontal and vertical directions does not affect the horizontal acceleration amplitude on the DSM. Figures 18b and 18c illustrate, respectively, the response spectrum and Fourier amplitude spectrum of vertical acceleration at the DSM (41.5 meters away; Point B) for unidirectional and bidirectional earthquake applications. When the earthquake is applied bidirectionally, the vertical acceleration on the DSM increases significantly across all frequencies. This increase in vertical acceleration, particularly at high frequencies, can significantly impact the seismic performance of power plant structures and the sensitive equipment they contain in near-fault regions.

5- 6- Additional assessment of DSM performance under Near-Fault events

To thoroughly assess how near-fault earthquakes affect the seismic performance of soil improved by the deep soil mixing (DSM) method, analyses used seven near-fault earthquake records (detailed in Table 7). In these analyses, the soil profile consisted of Nevada sand with a relative density of 60%—the improved soil layer measured 83 meters by 7.5 meters. The sand layer, measuring 400 meters by 150 meters, was analyzed under excitation in the x-direction for near-fault earthquakes. All analyses modeled the soil medium as an infinite domain to prevent unrealistic wave reflections. Figure 19 presents the horizontal acceleration response spectrum at the center of the DSM and the vertical acceleration response spectrum due to rocking motion at a distance of 41.5

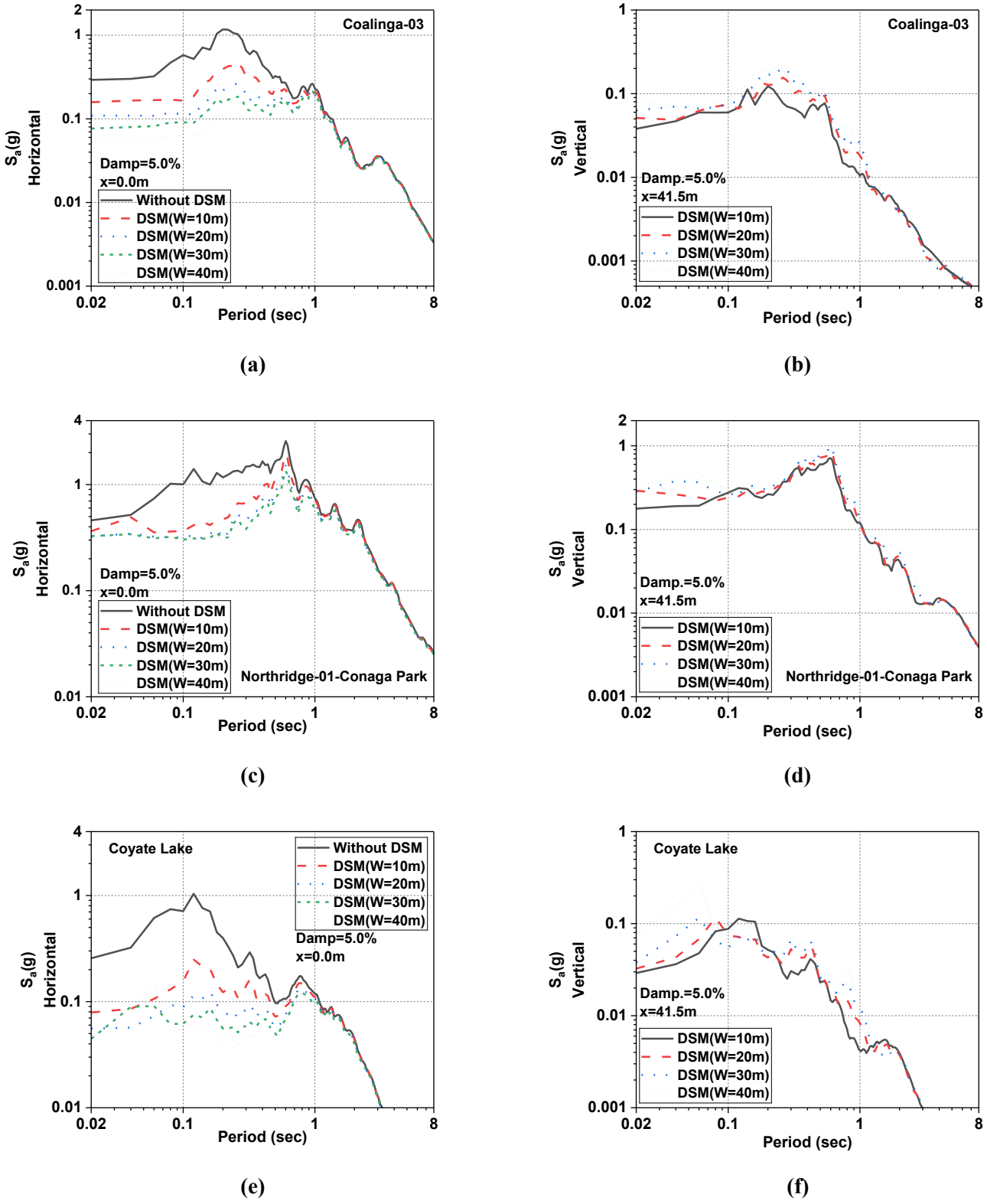

Fig. 19. Horizontal acceleration spectra at the center of the DSM block and vertical acceleration spectra induced by rocking motion at a distance of 41.5 m from the DSM center: (a, b) Coalinga-03 (1983); (c, d) Northridge-01 (1994), Canoga Park station; (e, f) Coyote Lake (1979); (g, h) Hollister-03 (1974); (i, j) Mammoth Lakes-07 (1980); (k, l) Oroville-03 (1975); (m, n) Northridge-01 (1994), Pardee station. (Continued)

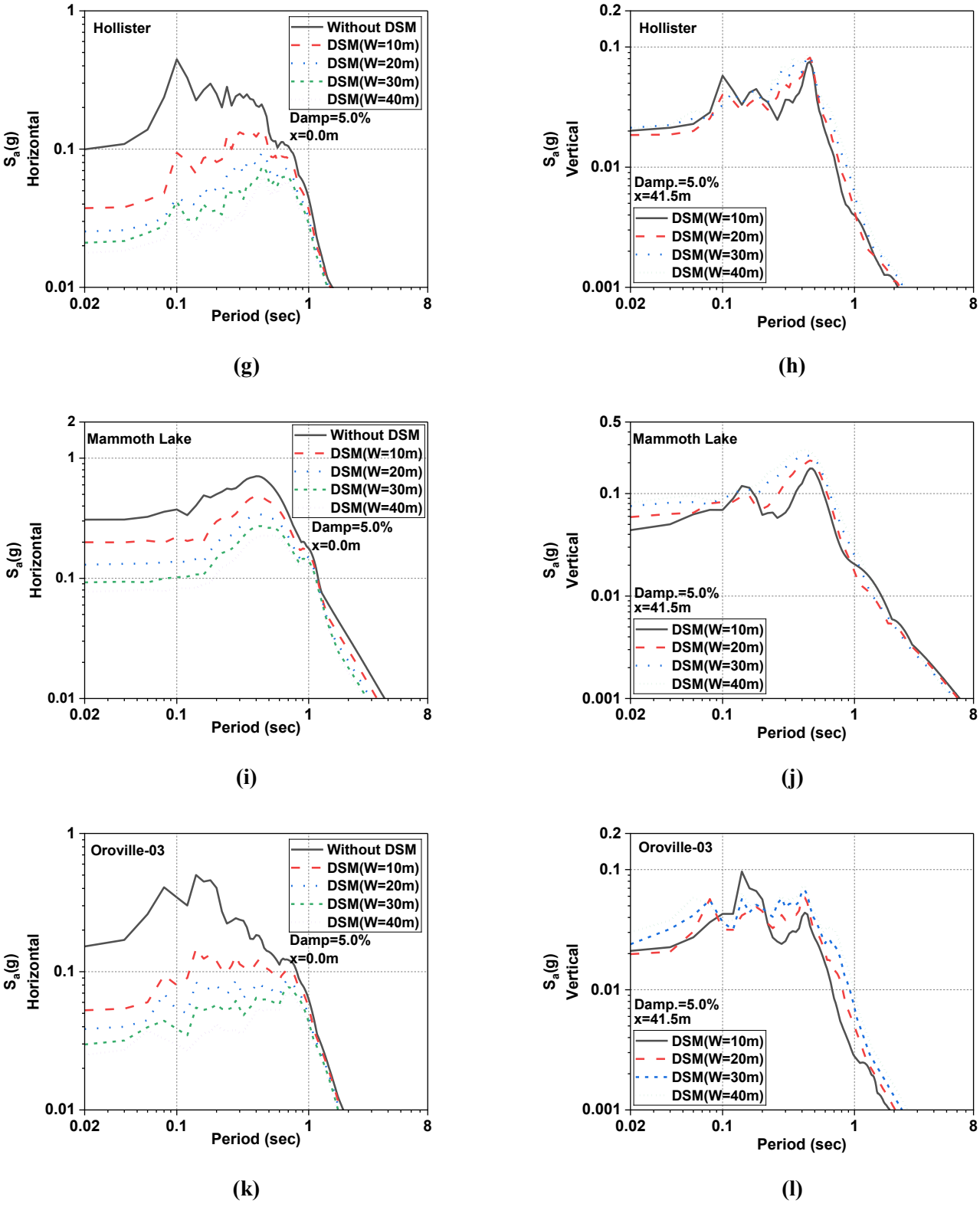

Fig. 19. Horizontal acceleration spectra at the center of the DSM block and vertical acceleration spectra induced by rocking motion at a distance of 41.5 m from the DSM center: (a, b) Coalinga-03 (1983); (c, d) Northridge-01 (1994), Canoga Park station; (e, f) Coyote Lake (1979); (g, h) Hollister-03 (1974); (i, j) Mammoth Lakes-07 (1980); (k, l) Oroville-03 (1975); (m, n) Northridge-01 (1994), Pardee station. (Continued)

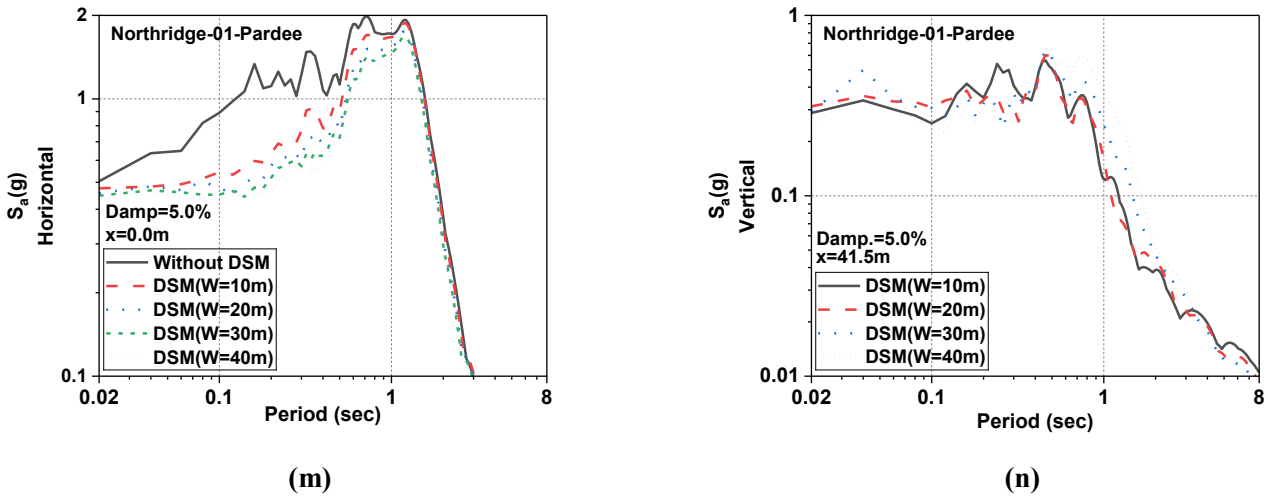

Fig. 19. Horizontal acceleration spectra at the center of the DSM block and vertical acceleration spectra induced by rocking motion at a distance of 41.5 m from the DSM center: (a, b) Coalinga-03 (1983); (c, d) Northridge-01 (1994), Canoga Park station; (e, f) Coyote Lake (1979); (g, h) Hollister-03 (1974); (i, j) Mammoth Lakes-07 (1980); (k, l) Oroville-03 (1975); (m, n) Northridge-01 (1994), Pardee station.

Table 7. The seismic event is considered in the present study.

Earthquake name(year)	Station name	M	V_{S30} (m/s)	R_{rup} (Km)	PGA (g)	PGA/PGV (s^{-1})	Type
Northridge-01(1994)	Pardee - SCE	6.69	325.67	5.54	0.55	7.1	Pulse
Hollister-03(1974)	San Juan Bautista	5.14	335.5	8.56	0.046	17	No Pulse
Northridge-01(1994)	Canoga Park	6.69	267.49	0	0.39	6.1	Double Pulse
Parkfield-02, CA (2004)	Parkfield - Cholame 1E	6	326.64	1.66	0.23	22.8	Pulse
Mammoth Lakes-07(1980)	Green Church	4.73	353.2	2.84	0.16	13.5	No Pulse
Oroville-03(1975)	Pacific Heights Rd (OR4)	4.75	352.22	8.7	0.067	20.3	No Pulse
Coalinga-03(1983)	Burnett Construction	5.38	352.2	12.89	0.167	23.4	No Pulse
Coyote Lake(1979)	Gilroy Array #3	5.74	349.85	6.75	0.15	20.5	Pulse

meters from the DSM center for each analysis. The results indicated that increasing the thickness of the improved layer reduces horizontal accelerations. However, as the DSM thickness increases, its effectiveness gradually diminishes. This finding suggests that while improved soil effectively reduces horizontal accelerations, excessive thickness does not necessarily guarantee enhanced performance. Regarding vertical acceleration caused by rocking motion, it was observed that for periods shorter than 0.1 seconds, increasing the DSM thickness results in higher vertical acceleration. Over the 0.1 to 1 second range, a more complex behavior was observed: in some cases, a thinner DSM layer led to greater vertical acceleration. For instance, in the Oroville-03 (1975) earthquake analysis, an improved soil layer 7.5 meters thick produced the highest vertical acceleration response due to rocking motion at 0.14 seconds. These results highlight the significance of soil-structure interaction and indicate that the impact of DSM on seismic response is not solely a function of its thickness but also depends on the soil's dynamic properties and the frequency content of the input earthquake motion.

6- Conclusion

This study examines the seismic performance of a Nevada sand layer under dry conditions and varying relative densities using two-dimensional OpenSees V3.5.0 modeling. The analysis is performed using near-field earthquake records, which include both pulse-type and non-pulse records. The PDMY02 constitutive model predicts sand behavior, and the Free Field boundary condition is applied to the lateral and bottom boundaries. All models are analyzed under horizontal ground motions induced by near-field earthquakes. The results show that:

1- The increase in the relative density of sand leads to a rise in the horizontal acceleration response, particularly in the higher frequency range. Examination of the Fourier amplitude spectrum of horizontal acceleration at the DSM during the Parkfield-02, CA (2004) earthquake revealed that, at frequencies below 0.6 Hz, changes in relative density did not affect the acceleration amplitude. However, denser sand resulted in lower acceleration amplitudes over the frequency range of 0.6-1 Hz. In comparison, at frequencies above 1 Hz, denser sand increased the acceleration amplitude. Additionally, the effect of relative density on rocking motion varied across different periods. In the vertical acceleration response spectrum, at periods shorter than 0.1 seconds and more prolonged than 0.2 seconds, an increase in relative density led to a reduction in the vertical acceleration due to rocking motion, whereas in the period range of 0.1 to 0.2 seconds, an increase in relative density caused an increase in rocking motion.

2- The analysis of dry Nevada sand with a relative density of 60% under the influence of eight near-field records revealed that at periods shorter than 0.1 seconds and longer than 0.3 seconds, an increase in the DSM thickness led to a rise in the vertical acceleration due to rocking motion. However, in the 0.1-0.3 second range, a thinner DSM resulted in higher vertical acceleration in some analyses. This highlights the importance of case-specific evaluation of the soil-DSM interaction tailored to each project's conditions.

3- The analysis results showed that increasing the thickness of the DSM reduces the horizontal acceleration response, particularly at high frequencies. Specifically, compared with the free-field horizontal acceleration, DSMs with different thicknesses yielded reductions of 27 percent at 10 meters, 38 percent at 20 meters, 43.5 percent at 30 meters, and 48.1 percent at 40 meters. However, this soil improvement method also led to increased vertical accelerations induced by rocking motion and steeper Arias intensity curves for horizontal accelerations on the DSM. On average, increasing the DSM thickness from 10 meters to 40 meters increased vertical accelerations by 76 percent for vibration periods below 2 seconds. As an initial assumption for determining DSM thickness, it is recommended to use a value equal to one-fifth of the shear wavelength in the soil layer. Nevertheless, the sensitivity of DSM rocking motion to the earthquake's frequency content and the soil's dynamic properties indicates that a case-specific evaluation of soil–DSM interaction is necessary for each project.

4- Increasing the width of the DSM had no significant effect on reducing horizontal accelerations, as DSM models with different widths (L = 21, 42, 62, 83 m) all reduced the horizontal acceleration amplitude at the ground surface by approximately 20% compared to the free-field response for vibration periods below 1 second. However, the analyses showed that increasing the DSM width significantly reduces vertical accelerations induced by rocking motion, particularly at high frequencies. Specifically, increasing the width from 21 to 42 m reduced the vertical acceleration amplitude by 42.36%, from 21 to 63 m by 63.45%, and from 21 to 83 m by 50% for vibration periods below 0.5 seconds. These findings indicate that increasing the DSM width can be an effective tool for controlling rocking motion in soil–structure systems. A wider DSM may lead to a more even distribution of seismic loads across soil layers, ultimately reducing the effects of rocking motion and the resulting vertical accelerations.

5- From the perspective of seismic performance and considering the potential reduction in implementation costs of block deep mixing (BDM), two alternative designs of toothed deep mixing were analyzed under a near-fault earthquake record. The results indicated that both alternatives, similar to conventional block deep mixing, significantly reduce horizontal accelerations. Specifically, compared to free-field ground response, for vibration periods below 1 second, the block deep mixing reduced the horizontal acceleration amplitude by 22.9%, toothed deep mixing Type 1 by 20.2%, and toothed deep mixing Type 2 by 21.1% at the ground surface. However, both alternative designs also increased the vertical accelerations induced by rocking motion, with the toothed deep-mix Type 1 and Type 2 designs raising them by 5.1% and 4.7%, respectively. This increase could have a notable impact on the performance of power plant structures and sensitive equipment located within them.

6- The analyses showed that applying the earthquake in a bi-directional manner leads to a significant increase in vertical acceleration on the DSM, with the amplitude of vertical acceleration increasing by more than eight times compared to the single-directional earthquake case. In contrast, the horizontal acceleration on the DSM does not change significantly relative to the single-directional case. These findings indicate that for sensitive structures with high-frequency content near a fault, the effects of bidirectional earthquake loading on vertical acceleration must be carefully considered, whereas changes in horizontal acceleration are of lesser concern.

7- The effects arising from soil–structure and structure–soil–structure interaction are highly case-specific, and the resulting behavior can vary significantly depending on project-specific factors such as the frequency content of the seismic input, the structural characteristics, and the soil layer properties. Therefore, the primary objective

of this study is to provide a general assessment of the seismic response of soil improved with Block-Type Deep Soil Mixing (BDSM) and to enhance the understanding of the dynamic behavior of soil–DSM systems. The recommendations presented in this work are intended solely as preliminary guidelines and should not be considered as definitive or universally applicable for all engineering projects.

7- Discussion

Tyapin's study on the seismic performance of Block-type Deep Soil Mixing (DSM, also known as Soil Pillows) demonstrated that the ratio of DSM thickness to the shear wave wavelength is a key parameter in controlling seismic response. Since the wavelength depends on the excitation frequency, the protective effectiveness of DSM is frequency-dependent. The present study confirms that increasing DSM thickness beyond one-fifth of the shear wavelength has no significant effect on reducing horizontal response, is not cost-effective, and can increase vertical accelerations due to rocking motion. Tiapin also showed that the protective effect of DSM on horizontal acceleration is largely independent of the horizontal dimensions of the improved zone, provided that these dimensions are sufficiently large relative to the layer thickness to prevent severe rocking—a finding corroborated in this research. Furthermore, DSM's effect on vertical accelerations primarily stems from the mass of the superstructure. In the present study, without considering the structure and under near-fault bidirectional loading, DSM was found to have a negligible impact on reducing vertical accelerations. [64, 65]. Similarly, Moradi et al. [18] reported that Block-type DSM can significantly reduce horizontal ground accelerations. In models subjected to artificial excitations based on a Uniform Hazard Spectrum, horizontal acceleration reductions ranged from 45% to 60%, whereas real earthquake records yielded reductions of 22% to 50%. The current study confirms these findings, showing that increasing the DSM thickness from 5 m to 40 m substantially reduces horizontal acceleration relative to free-field conditions. The protective effectiveness of DSM becomes pronounced only when the stiffness contrast between the improved soil and the surrounding natural soil is sufficiently high.

References

[1] J. Puppala Anand, A. Porbaha, V. Bhadriraju, E. Wattanasanthichareon, In Situ Test Protocols for Quality Assessments of Deep Mixing Columns, in: Geotechnical Engineering for Transportation Projects, 2012, pp. 1429-1438.

[2] S. Madhyannapu Raja, J. Puppala Anand, S. Nazarian, D. Yuan, Quality Assessment and Quality Control of Deep Soil Mixing Construction for Stabilizing Expansive Subsoils, Journal of Geotechnical and Geoenvironmental Engineering, 136(1) (2010) 119-128.

[3] R.S. Madhyannapu, A.J. Puppala, Design and Construction Guidelines for Deep Soil Mixing to Stabilize Expansive Soils, Journal of Geotechnical and Geoenvironmental Engineering, 140(9) (2014) 04014051.

[4] P.T.A. Vu, Ground improvement using soil-cement method: a case study with laboratory testing and in-situ verification for a highway project in southern Vietnam, Geotechnical Engineering Journal of the SEAGS & AGSSEA, 47(1) (2016) 45-49.

[5] M. Kitazume, M. Terashi, The deep mixing method, CRC Press, 2013.

[6] D.A. Bruce, Introduction to the Deep Mixing Methods as Used in Geotechnical Applications. Volume 3: The Verification and Properties of Treated Ground, (2001).

[7] D.A. Bruce, E. Geosystems, An introduction to the deep soil mixing methods as used in geotechnical applications, United States. Federal Highway Administration. Office of Infrastructure …, 2000.

[8] T. Edil, D. Staab, Practitioner's guide for deep-mixed stabilization of organic soils and peat, Final Report, The National Deep Mixing Research Program, Project Number NDM302, (2005) 60.

[9] P.G. Nicholson, Soil improvement and ground modification methods, Butterworth-Heinemann, 2014.

[10] P.J.V. Oliveira, J.L. Pinheiro, A.A. Correia, Numerical analysis of an embankment built on soft soil reinforced with deep mixing columns: Parametric study, Computers and Geotechnics, 38(4) (2011) 566-576.

[11] J.-J. Chen, L. Zhang, J.-F. Zhang, Y.-F. Zhu, J.-H. Wang, Field Tests, Modification, and Application of Deep Soil Mixing Method in Soft Clay, Journal of Geotechnical and Geoenvironmental Engineering, 139(1) (2013) 24-34.

[12] G. Spagnoli, E. Salvatore, M. Arciero, G. Modoni, Improving the Performance of Deep Soil Mixing in Clay with Chemical Additives, in: Geo-Congress 2022, pp. 186-195.

[13] A. Ter-Martirosyan, V. Sidorov, E. Sobolev, Dynamic Properties of Soil Cements for Numerical Modelling of the Foundation's Basis Transformed under the Technology of Deep Soil Mixing: A Determination Method, Buildings, 12(7) (2022) 1028.

[14] X. Zhang, H. Zhu, Z. Jiao, Z. Cen, Lattice-shaped ground improvement by mixing soil and alkali-activated slag for liquefaction mitigation, Case Studies in Construction Materials, 17 (2022) e01445.

[15] F. Wang, K. Li, Y. Liu, Optimal water-cement ratio of cement-stabilized soil, Construction and Building Materials, 320 (2022) 126211.

[16] S.-L. Shen, J. Han, Y.-J. Du, Deep mixing induced property changes in surrounding sensitive marine clays, Journal of Geotechnical and Geoenvironmental Engineering, 134(6) (2008) 845-854.

[17] S. Larsson, M. Dahlström, B. Nilsson, Uniformity of lime-cement columns for deep mixing: a field study, Proceedings of the Institution of Civil Engineers- Ground Improvement, 9(1) (2005) 1-15.

[18] M.M. Shaghaghi, I.M. Kani, H. Yousefi, The Seismic

Behavior of Block Type Deep Soil Mixing, Latin American Journal of Solids and Structures, 18 (2021).

[19] T.S. To, H.L. Minh, T.Q. Huynh, S. Khatir, M.A. Wahab, T. Cuong-Le, A nonlinear optimization method for calibration of large-scale deep cement mixing in very soft clay deep excavation, International Journal for Numerical and Analytical Methods in Geomechanics, 48(8) (2024) 1949-1978.

[20] A. Hasheminezhad, H. Bahadori, Shallow foundations subjected to earthquake-induced soil liquefaction resting on deep soil mixing columns, Innovative Infrastructure Solutions, 8(5) (2023) 145.

[21] B. Ramezani, H. Dehghan Khalili, P. Moradi, A. Pourbagheri, Seismic Resilience with Deep Soil Mixing: Numerical and Experimental Insights into Liquefaction Mitigation, Geotechnical and Geological Engineering, 43(2) (2025) 71.

[22] B.A. Bradley, K., Araki, T., Ishii, K., Saitoh, Effect of lattice-shaped ground improvement geometry on seismic response of liquefiable soil deposits via 3-D seismic effective stress analysis, Soil Dynamics and Earthquake Engineering, 48 (2013) 35-47.

[23] P. Moradi, H.D. Khalili, M.R. Arvin, Deep Soil Mixing Columns as Settlement-Reducing Elements in Sandy Soils: A Numerical Study, International Journal of Geomechanics, 23(4) (2023) 04023015.

[24] S.-Y. Liu, Y.-J. Du, Y.-L. Yi, A.J. Puppala, Field investigations on performance of T-shaped deep mixed soil cement column–supported embankments over soft ground, Journal of Geotechnical and Geoenvironmental Engineering, 138(6) (2012) 718-727.

[25] T. Namikawa, J. Koseki, Y. Suzuki, Finite element analysis of lattice-shaped ground improvement by cement-mixing for liquefaction mitigation, Soils and Foundations, 47(3) (2007) 559-576.

[26] M. Khosravi, W. Boulanger Ross, S. Tamura, W. Wilson Daniel, C.G. Olgun, Y. Wang, Dynamic Centrifuge Tests of Soft Clay Reinforced by Soil–Cement Grids, Journal of Geotechnical and Geoenvironmental Engineering, 142(7) (2016) 04016027.

[27] A. Yaghfoori, I. Mahmoudzadeh Kani, H. Yousefi, Seismic performance and optimization of deep soil mixing (DSM) for response mitigation at power plant sites, Engineering Computations, (2025) 1-42.

[28] A. Elgamal, J. Lu, D. Forcellini, Mitigation of Liquefaction-Induced Lateral Deformation in a Sloping Stratum: Three-dimensional Numerical Simulation, Journal of Geotechnical and Geoenvironmental Engineering, 135(11) (2009) 1672-1682.

[29] M.K. Alhamdi, B.S. Albusoda, A Review on Deep mixing method for soil improvement, IOP Conference Series: Materials Science and Engineering, 1105(1) (2021) 012110.

[30] H. Yang, Y. Li, W. Pan, L. Hu, S. Ji, Automatic classification of near-fault pulse-like ground motions, Computer-Aided Civil and Infrastructure Engineering, 40(11) (2025) 1490-1507.

[31] J. Feng, B. Zhao, Z. Wang, Single-pulse-like and double-pulse-like characteristics of near-fault ground motions, Soil Dynamics and Earthquake Engineering, 177 (2024) 108438.

[32] G. Chen, J. Yang, R. Wang, K. Li, Y. Liu, M. Beer, Seismic damage analysis due to near-fault multipulse ground motion, Earthquake Engineering & Structural Dynamics, 52(15) (2023) 5099-5116.

[33] F. McKenna, G.L. Fenves, The OpenSees command language manual, University of California, Berkeley (opensees. ce. berkeley. edu), (2001).

[34] R. Ribó, M. Pasenau, E. Escolano, J. Ronda, L. González, GiD reference manual, CIMNE, Barcelona, 27 (1998) 25.

[35] S. Mazzoni, F. McKenna, M.H. Scott, G.L. Fenves, Open system for earthquake engineering simulation user command-language manual, Report NEES grid-TR 2004, 21 (2006).

[36] Z. Yang, Numerical modeling of earthquake site response including dilation and liquefaction, Columbia University, 2000.

[37] A. Elgamal, Z. Yang, E. Parra, A. Ragheb, Modeling of cyclic mobility in saturated cohesionless soils, International Journal of Plasticity, 19(6) (2003) 883-905.

[38] Z. Karimi, S. Dashti, Seismic performance of shallow-founded structures on liquefiable ground: validation of numerical simulations using centrifuge experiments, Journal of Geotechnical and Geoenvironmental Engineering, 142(6) (2016) 04016011.

[39] S.L. Kramer, J.P. Stewart, Geotechnical earthquake engineering, CRC Press, 2024.

[40] F.-Y. Menq, Dynamic properties of sandy and gravelly soils, The University of Texas at Austin, 2003.

[41] C. Phillips, Y.M. Hashash, S.M. Olson, M.R. Muszynski, Significance of small strain damping and dilation parameters in numerical modeling of free-field lateral spreading centrifuge tests, Soil Dynamics and Earthquake Engineering, 42 (2012) 161-176.

[42] T. Kokusho, T. Aoyagi, A. Wakunami, In situ soil-specific nonlinear properties back-calculated from vertical array records during 1995 Kobe Earthquake, Journal of Geotechnical and Geoenvironmental Engineering, 131(12) (2005) 1509-1521.

[43] D. Park, Y.M. Hashash, Evaluation of seismic site factors in the Mississippi Embayment. II. Probabilistic seismic hazard analysis with nonlinear site effects, Soil Dynamics and Earthquake Engineering, 25(2) (2005) 145-156.

[44] Y. Deng, S. Dashti, A. Hushmand, C. Davis, B. Hushmand, Seismic response of underground reservoir structures in sand: evaluation of class-c and c1 numerical

simulations using centrifuge experiments, Soil Dynamics and Earthquake Engineering, 85 (2016) 202-216.

[45] Z. Karimi, S. Dashti, Seismic performance of structures on liquefiable soils: insight from numerical simulations and centrifuge experiments, J Geotech Geoenviron Eng ASCE, (2016).

[46] C.A.d. Moura, C.S. Kubrusly, The Courant-Friedrichs-Lewy (CFL) condition: 80 years after its discovery, Birkhäuser Basel, 2012.

[47] L. Cruz, M.I. Todorovska, M. Chen, M.D. Trifunac, A. Aihemaiti, G. Lin, J. Cui, The role of the foundation flexibility on the seismic response of a modern tall building: Vertically incident plane waves, Soil Dynamics and Earthquake Engineering, 184 (2024) 108819.

[48] B. Jeremić, G. Jie, M. Preisig, N. Tafazzoli, Time domain simulation of soil–foundation–structure interaction in non-uniform soils, Earthquake Engineering & Structural Dynamics, 38(5) (2009) 699-718.

[49] A.S.o.C. Engineers, Seismic analysis of safety-related nuclear structures and commentary, in American Society of Civil Engineers, 2000.

[50] P.A. Amalu, B.R. Jayalekshmi, Study on seismic response of unconnected piled raft with rubber mixed soil, Materials Today: Proceedings, (2023).

[51] O. Çetindemir, A.C. Zülfikar, Numerical validation of fully coupled nonlinear seismic soil–pile–structure interaction, Buildings, 14(6) (2024) 1502.

[52] A.H. Nielsen, Absorbing boundary conditions for seismic analysis in ABAQUS, in: ABAQUS users' conference, 2006, pp. 359-376.

[53] M.R. Islam, S.D. Turja, D. Van Nguyen, D. Forcellini, D. Kim, Seismic soil-structure interaction in nuclear power plants: An extensive review, Results in Engineering, 23 (2024) 102694.

[54] C. Kanellopoulos, P. Rangelow, B. Jeremic, I. Anastasopoulos, B. Stojadinovic, Dynamic structure-soil-structure interaction for nuclear power plants, Soil Dynamics and Earthquake Engineering, 181 (2024) 108631.

[55] D. Van Nguyen, D. Kim, D. Duy Nguyen, Nonlinear seismic soil-structure interaction analysis of nuclear reactor building considering the effect of earthquake frequency content, Structures, 26 (2020) 901-914.

[56] A.G. Sextos, G.D. Manolis, A. Athanasiou, N. Ioannidis, Seismically induced uplift effects on nuclear power plants. Part 1: Containment building rocking spectra, Nuclear Engineering and Design, 318 (2017) 276-287.

[57] N. Saxena, D. Paul, R. Kumar, Effects of slip and separation on seismic SSI response of nuclear reactor building, Nuclear Engineering and Design, 241(1) (2011) 12-17.

[58] N. Saxena, D.K. Paul, Effects of embedment including slip and separation on seismic SSI response of a nuclear reactor building, Nuclear Engineering and Design, 247 (2012) 23-33.

[59] T. Gupta, M.K. Annam, Free Field Plane Strain Simulation of Soil Liquefaction Using Finite Element Analysis, Indian Geotechnical Journal, 54(5) (2024) 2033-2044.

[60] A. Khosravifar, A. Elgamal, J. Lu, J. Li, A 3D model for earthquake-induced liquefaction triggering and post-liquefaction response, Soil Dynamics and Earthquake Engineering, 110 (2018) 43-52.

[61] A.S.o.C. Engineers, Seismic analysis of safety-related nuclear structures, in American Society of Civil Engineers, 2017.

[62] D.A. Bruce, M.E.C. Bruce, A.F. DiMillio, Deep mixing method: A global perspective, Geotechnical special publication, (1998) 1-26.

[63] G. Mullins, M. Gunaratne, K. Johnson, K. Costello, S. Baker, E. Mitchell, J. Vomacka, M. Mullins, Soil mixing design methods and construction techniques for use in high organic soils, (2015).

[64] A. Tyapin, Effect of soil improvement on seismic response, (2017).

[65] A. Tyapin, S. Halil, Soil-structure interaction, ISBN, 2012.

HOW TO CITE THIS ARTICLE

A. Yaghfoori, I. Mahmoudzadeh Kani, H. Yousefi, Seismic Behavior of Dry Sandy Soils Improved with Block-Type Deep Soil Mixing in Near-Fault Regions, AUT J. Civil Eng., 10(1) (2026) 25-48.

DOI: 10.22060/ajce.2025.24157.5923